CrystEngComm

Accepted Manuscript

This article can be cited before page numbers have been issued, to do this please use: L. Yu, H. You, Q. Zhang, L. Zhang and J. Fang, *CrystEngComm*, 2019, DOI: 10.1039/C8CE02041H.

ROYAL SOCIETY OF CHEMISTRY

rsc.li/crystengcomm

ROYAL SOCIETY OF CHEMISTRY
View Article Online
DOI: 10.1039/C8CE02041H

Journal Name

COMMUNICATION

Digestive Ripening Mechanism Investigation in a Classical Lee-Meisel Method based on *in situ* UV–vis spectra

Received 00th January 20xx,
Accepted 00th January 20xx

DOI: 10.1039/x0xx00000x

www.rsc.org/

Liang Yu,[a] Hongjun You,*[a,b] Qifan Zhang,[b] Lingling Zhang,[b] and Jixiang Fang*[b]

Uniform spherical Ag NPs with controllable size are synthesized in a simple one-step aqueous solution system. A unique digestive ripening process is observed using *in situ* UV-vis spectra, which performs key functions for the formation of ultra-uniform Ag NPs.

Colloidal noble metal nanoparticles (NPs), especially of silver and gold, have drawn great of interest as good candidates for applications in plasmonics,[1] surface enhanced Raman scattering,[2] chemical and biological sensing,[3] and chemical catalysis.[4,5] The attractive applications of noble metal NPs are usually based on the surface plasmon resonance (SPR).[6] It has been realized that the shape and size of noble metal NPs play important roles in determining the plasmon properties. Great interest has been stimulated in the shape-controlled synthesis of noble metal NPs and various shapes, including sphere,[7] cubes,[8] polyhedrons,[9] plates,[10] wires,[11] and hierarchical shapes,[12] have been obtained with tunable SPR wavelength. In principle, the plasmon band of the noble metal NPs can be systematically tuned by controlling the shape and size. To obtain the desired NPs, in most cases, all kinds of synthetic conditions, including the concentrations of reagents, surfactants, temperature, reaction time, and so on, should be finely tuned. The nucleation and growth of NPs always are very sensitive to the small variations of synthetic conditions, which may lead to poor predictability and low reproducibility in the synthesis of noble metal NPs.

It is no exception for the synthesis of Ag NPs. The spherical Ag NPs are the generally applied and studied nanostructure in optical field, which also can be employed as seeds or templates to synthesize much more complex nanostructures.[13-15] Although people have possible to obtain spherical Ag NPs with size within a considerable range through controlling the synthesis conditions, at present, tailored synthesis of NPs with finely tuned size and very uniform shape using a simple synthesis system is still a great challenge. During the growth stage of colloid metal NPs, Ostwald ripening is always happened and induces the growth of large NPs and the shrink of small NPs, thus results in the non-uniform distribution of NPs size.[16] People have developed many strategies such as burst nucleation,[16] surface stabling with capping agents,[17,18] and so on, to inhibit the Ostwald ripening. On the other hand, digestive ripening is a unique synthetic process that is converse to Ostwald ripening and leads to the conversion of polydisperse NPs into uniform monodisperse ones.[19] Different with the Ostwald ripening process, the digestive ripening process includes the dissolution or etching of the large NPs using excess strongly coordinating ligands and the growth of small NPs by the expense of large ones.[20] However, state-of-the-art digestive ripening process is mainly successfully performed in the synthesis of hydrophobic noble metal NPs by using strongly coordinating agents such as amines, alkylthiols, and phosphines as surfactant ligands.[21] Correspondingly, the synthesis solutions are nonpolar solvent such as chloroform, benzene, toluene or dichlorobenzene.[18] The surficial significant passivation and insolubility of the produced noble-metal NPs in many polar solvent greatly limit their use in many applications. Thus it makes more sense in practical application to develop a process in which mild ligands are employed as they can be removed easily.

In this study, very uniform Ag NPs are synthesized in a simple aqueous solution by taking advantage of the digestive ripening process. The method and strategy are based on the classical Lee-Meisel synthesis method for Ag NPs, which avoid the using of strongly coordinated hydrophobic ligands and thus enable us to obtain monodisperse Ag NPs with exchangeable and hydrophilic surface. At the same time, the size of Ag NPs can be continuously tuned from 25 nm to 60 nm. As a proof-of-concept, we demonstrate for the first time that hydrophilic monodisperse Ag NPs could be synthesized in aqueous solution without employing special ligands and additional oxidative etching agents. Thus, this novel system provides a robust method to synthesize water-soluble spherical

[a] School of Science, Xi'an Jiaotong University, Xi'an, Shaanxi 710049, China
[b] China Key Laboratory of Physical Electronics and Devices of Ministry of Education, School of Electronic and Information Engineering, Xi'an Jiaotong University, Xi'an, Shaanxi 710049, China

Electronic Supplementary Information (ESI) available: Experimental detail, FDTD simulation method and MD simulation method. See DOI: 10.1039/x0xx00000x

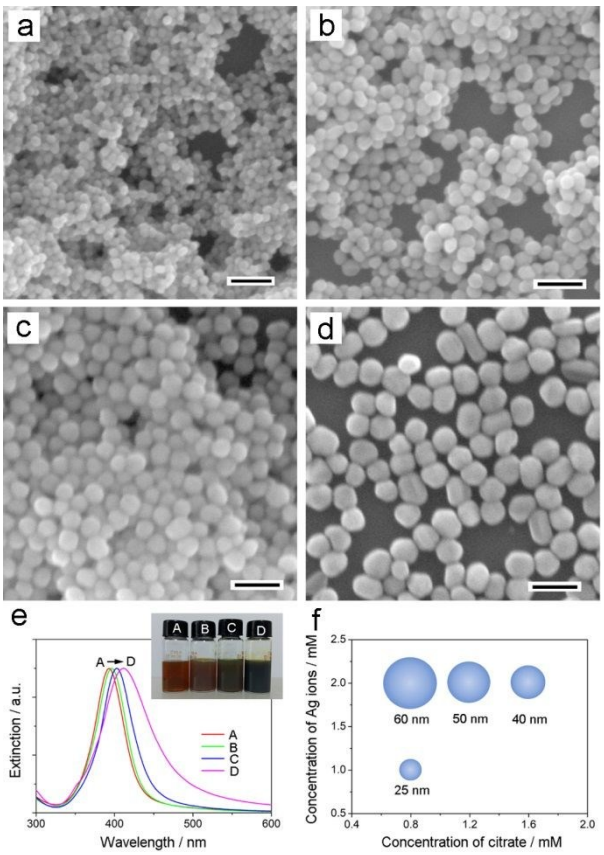

Fig. 1 Morphology and extinction spectra of the Ag NPs with different sizes. (a-d) SEM images of the spherical Ag NPs with average sizes: 25 nm, 40 nm, 50 nm, and 60 nm, respectively. The scale bars in (a-d) are 100 nm. (e) UV-vis extinction spectra of the Ag NPs with 25 nm (A), 40 nm (B), 50 nm (C), and 60 nm (D). The inset is the photograph of aqueous solution containing Ag NPs. (f) Transformation of Ag NP size with different synthesis conditions.

monodisperse Ag NPs with high yield and uniform size, which has broaden its applications. We believe that the study of digestive ripening in this work also will enhance people's understanding and broaden its application for the control in the synthesis of colloid NPs.

Fig. 1 shows the morphology and ultraviolet-visible (UV-vis) spectra of Ag NPs that are obtained in our synthesis system based on Lee-Meisel method. The Lee-Meisel method is the classic method to synthesize Ag NPs by reducing $AgNO_3$ with sodium citrate in an aqueous solution and now is widely used in the preparation of quasi-spherical Ag NPs.[22,23] However, this simple method tends to produce a large variety of sizes and a diversity of shapes in a single reaction. To prevent the oxidation of Ag NP, the synthesis process is usually performed in nitrogen or argon condition. Different with conventional Lee-Meisel method, we performed the synthesis in air condition. Typically, a sodium citrate aqueous solution was injected into the boiling $AgNO_3$ aqueous solution and the sphere Ag NPs were obtained after 30 min. The experimental detail is shown in Supporting Information. This synthesis system is very simple, in which only two agents: $AgNO_3$ and sodium citrate. The Ag ions are metal precursor and the citrate ions perform as both reducing agent and surface ligand.

Fig. 1a is the scanning electron microscope (SEM) image of Ag NPs. It can be clearly seen that the Ag NPs are very uniform in spherical shape and size. More than 99% Ag NPs are spherical shape. The average size is around 25 nm with a narrow distribution. The standard deviation is only 1.8 nm. Through changing the synthesis conditions, such as concentration of Ag ions and citrate ions, the size of spherical Ag NPs can be successfully tuned. Figs. 1b-d show the SEM images of obtained Ag NPs with average sizes of 40 nm, 50 nm, and 60 nm, respectively. Similar with the 25 nm Ag NPs, these Ag NPs are also very uniform in shape and distribution.

The optical properties of obtained Ag NPs with different sizes are investigated by UV-vis spectroscopy. Fig. 1e shows the experimentally measured optical extinction spectra of Ag NPs dispersed in water solutions. The monodispersity of the Ag NPs allows the observation of well-defined extinction peak for the single Ag NP plasmon mode. For the spherical NPs, only one peak corresponding to the one mode of plasmon resonance is observed. The center of the extinction band locates at 393 nm with a very narrow half-peak breadth (only 39 nm) for the 25 nm Ag NPs. The narrow half-peak breadth further indicates that the shape and size of the NPs are very uniform. With the size of Ag NPs increasing from 25 nm to 40 nm, 50 nm, and 60 nm, the solution colour of the Ag NPs changes from orange to brick red, dark brick red, and dark brown, as shown in the inset of Fig. 1e. Correspondingly, the extinction bands of the dispersed Ag NPs transform from 393 nm to 397 nm, 404 nm, and 412 nm with the increase of NPs size.

In our experiment, the size of Ag NPs was tuned by changing the concentrations of Ag precursor and citrate ions. As shown in Fig. 1f, when the concentration of Ag ions is kept at 2 mM and the concentration of citrate ions is increased from 0.8 mM to 1.2 mM and 1.6 mM, the size of Ag NPs decrease from 60 nm to 50 nm and 40 nm. The increase of citrate ions will speed up the reducing rate. Thus, plenty of Ag atoms will be quickly produced at the nucleation stage, inducing the formation of more nucleuses as described by LaMer curve.[16] As the surface ligand, the citrate ions will further stabilize the produced Ag nucleuses. Thus greatly increased Ag NPs will be produced. Because the total amount of Ag precursor is constant, the amount of Ag atoms separated to single NP will decrease. Finally, the size of Ag NPs could be tuned to small by increasing of citrate ions. Similarly, if the concentration of citrate ions is kept constant, the Ag NP size also can be tuned by changing of the Ag precursor amount. Therefore, Ag NPs were changed from 60 nm to 25 nm as the decreasing of Ag ions concentration from 2 mM to 1 mM.

Besides of the tuning of size, the more important specialty of our modified Lee-Meisel synthesis method for Ag NPs is the controllability to the ultra-uniform size and shape. To investigate the mechanism of the shape control in this system, the growth process of the 25 nm Ag NPs are monitored by *ex situ* TEM/SEM observation. Figs. 2a-d show the TEM images of Ag NPs obtained with reaction times of 5 min, 10 min, 15 min, and 20 min. As shown in Fig. 2a, at the start stage, Ag NPs with a broad size distribution are produced. Following, the population of the large Ag NPs is significantly reduced, resulting in a decrease in the mean size of the NPs and a significant narrowing of the size distribution. The prolonged

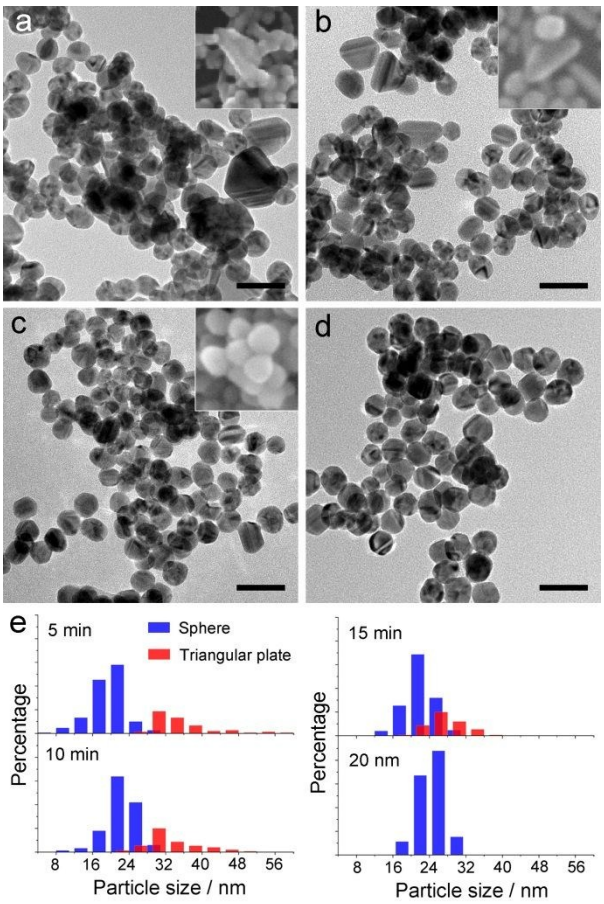

Fig. 2 Digestive ripening process of Ag NPs. (a-d) TEM, SEM (inset) images and (e) statistic size distributions of Ag NPs obtained with the reaction times: 5 min, 10 min, 15 min, and 20 min, respectively. The scale bars in (a-d) are 100 nm.

reaction time promotes the further narrowing of the size distribution (Figs. 2b and c). The ultra-uniform monodisperse Ag nanospheres are eventually obtained (Fig. 2d). Combined with the SEM image, it can be found that the large NPs in the start stage are triangular nanoplates (inset of Fig. 2a). With the prolonging of reaction time, the angles of the triangular nanoplates are gradually etched and their shapes correspondingly transform to near sphere (insets of Figs. 2b and c). This growth process disclosed by the TEM and SEM images displays a typical of a digestive ripening phenomenon.

Fig. 2e summarizes the size distributions of Ag NPs during the digestive ripening process. In this process, the size of triangular nanoplates is reduced by the etching and simultaneously the size of spherical NPs increase gradually. With the increase of the spherical NPs, the size distributions which start from a high standard deviation of 9.2 nm undergo a continuous decrease during the digestive ripening process. Finally, the standard deviation is reduced to 1.8 nm, confirming the excellent monodispersity of the obtained spherical Ag NPs.

From the SEM images (insets of Figs. 2a-c), we can notice that the triangular nanoplates show different surficial roughness during the growth process. At the start stage, the surface of the triangular nanoplates is coarse (inset of Fig. 2a). At the same time, some agglomeration of NPs also can be found in this system. In the later stage, the agglomeration of

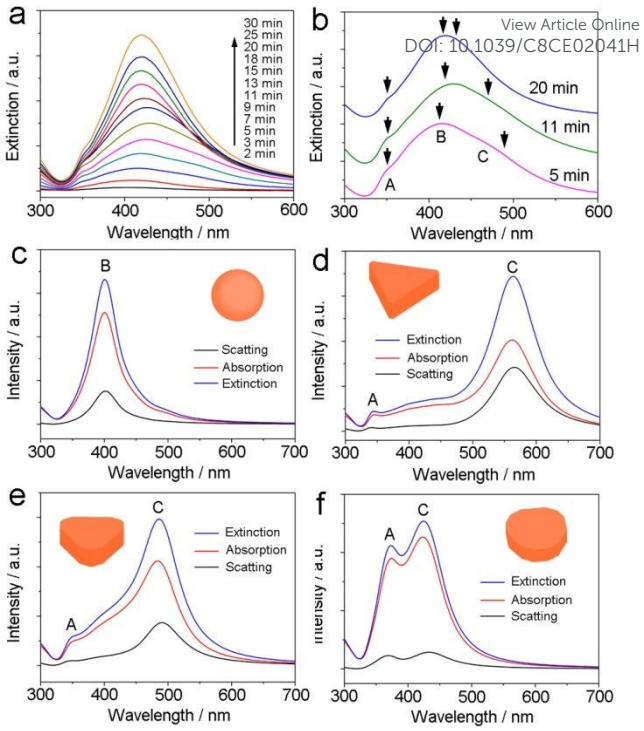

Fig. 3 UV-vis spectra of Ag NPs with different reaction times. (a) *In situ* UV-vis spectra of Ag NPs during the synthesis process at different reaction time. (b) The analysis for the selected UV-vis spectra of Ag NPs with reaction times: 5 min, 11 min, and 20 min. (c-f) Theoretically simulated spectra of Ag NPs with different morphologies.

NPs disappears and the surface of the triangular nanoplates becomes smooth. A possible coalescence process may be deduced from this phenomenon. At the start stage, after a burst nucleation process, initial non-uniform Ag NPs are produced. Following, the small Ag NPs aggregate to form triangular agglomeration through the particle-mediated growth mode.[16,24,25] Subsequently, based on the Ostwald ripening mechanism, the atom diffusion on the surface of triangular agglomeration which surface transform from coarse to smooth.[26,27]

The digestive ripening process of the Ag nanospheres was also monitored by the in situ UV-vis spectroscopy. As shown in Fig. 3a, with the Ag precursor being reduced and transformed into NPs, the intensity of extinction band is raised. A typical extinction spectra at 5 min reaction time shows three peaks, as labeled with A, B, and C in Fig. 3b. In the whole process, theposition of peak A is kept almost no change, peak B is red-shifted a little, and peak C is blue-shifted and finally merged with peak B. Figs. 3c-f are the corresponding simulated optical spectra of Ag NPs using the finite-difference time-domain (FDTD) method. Fig. 3c shows the simulated scatting, absorption and extinction spectra of 25 nm spherical Ag NPs. Only one peak is observed and located at 399 nm. For the triangular Ag nanoplate with 25 nm thickness and 60 nm length of side, the simulated extinction band shows two peaks. One is located at near to 350 nm and keeps no shift, the other one is blue-shifted with the angles of triangular nanoplates being gradually etched. Thus, we can attribute peak A and C in the experimental spectra to the triangular nanoplates and peak B can be attribute to nanosphere. This monitoring of the

View Article Online
DOI: 10.1039/C8CE02040H

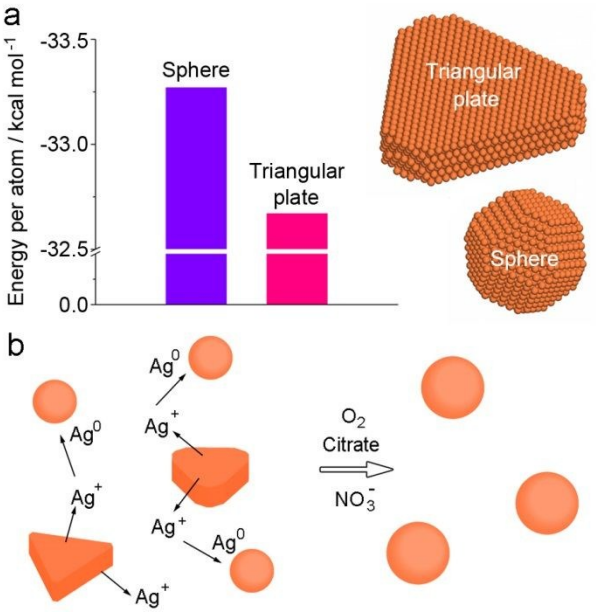

Fig. 4 Mechanism of the morphology transformation of Ag NPs. (a) Energy per atom in triangular nanoplate and nanosphere obtained with molecular dynamic (MD) simulation. (b) Schematic image illustrating the formation mechanism of uniform monodisperse Ag NPs by the digestive ripening.

in situ UV-vis spectroscopy also disclose the same digestive ripening process with that found in TEM/SEM observation.

The mechanism of digestive ripening was further studied using the molecular dynamics simulation (MD). Two kind of Ag NPs including spherical NP with size of 3 nm (containing 1673 Ag atoms) and angle-truncated triangular nanoplates with thickness of 2 nm and side length of 8 nm (containing 3625 Ag atoms) were built as simulation modes (inset of Fig. 4a). Depending on the previous report,[28,29] noble metal NPs are usually bounded by (111) and (100) crystalline planes with the lowest surface energy. Thus, Ag NP mode for the MD simulation is truncated octahedron which is covered by (111) and (100) planes. The angle-truncated triangular Ag nanoplate mode for the MD simulation is mainly covered by (111) plane on the top and bottom surface. The configurations of these modes were firstly optimized using MD method (same with our previous report, and detail is shown in Supporting Information).[30,31] As shown in Fig. 4a, after optimization, the atoms in spherical Ag NP possess even lower energy than that in triangular nanoplate, indicating that the spherical NP are more stable than the triangular nanoplate.

Therefore, based on the combination result of experiment and theoretical simulation, a reasonable mechanism can be proposed to describe this unique digestive ripening process. As illustrated by the schematic image in Fig. 4b, in the start stage of the synthesis, the Ag precursor is quickly reduced and forms two kinds of NPs, i.e. spherical NP and triangular nanoplate, after a burst nucleation process. Different with conventional Lee-Meisel synthesis method, the oxygen in the air is introduced into the reaction solution in our new method. At high reaction temperature, the introduction of oxygen combined with NO_3^- ions and citrate ions will performs oxidative etching to the Ag NPs. Compared with spherical NPs, the unstable triangular nanoplates are preferentially etched. During the etching process, the atoms located at corner are more unstable and are gradually etched, companied with the shape transform from triangular nanoplate to near sphere. At the same time, the concentration balance of Ag ions in the reaction solution will be destroyed by the increased Ag ions from the etching process, resulting in the regrowth of spherical Ag NPs as described by LaMer curve theory.[16] Finally, the ultra-uniform spherical Ag NPs are obtained through the digestive ripening process.

The properties of nanoscale metals are determined by a set of physical parameters that include composition, structure, shape and size. People have developed a plenty of method to obtain the metal NPs with various physical parameters.[32,33] Further, the uniformity of metal NPs is the other important issues should be well controlled. Here, just by modifying the synthesis conditions, the size of Ag NPs become obviously uniform. Compared with other well-established methods,[32,33] this strategy is very simple but effective.

In conclusion, monodisperse Ag nanospheres with ultra-uniform shape and size are synthesized using a modified Lee-Meisel method. The size of Ag nanospheres can be continuously tuned from 25 nm to 60 nm by changing the concentrations of Ag precursor and citrate ions. Through *ex situ* TEM/SEM and *in situ* UV-vis spectroscopy monitoring to the growth of Ag NPs, a unique digestive ripening process was fund and displays key roles in the transformation of Ag NPs from polydisperse to monodisperse. FTDT and MD simulation results further disclose the mechanism of oxygen mediated digestive ripening process in this modified Lee-Meisel synthesis system. We believe that this study not only provides a new robust strategy for the synthesis of monodisperse Ag NPs, but also helps to deeply understanding of the unique digestive ripening process that remains elusive to date.

Acknowledgements

This work was supported by the Natural Science Foundation of Shaanxi Province (No. 2017JM5072), the National Natural Science Foundation of China (Nos. 21675122, 21874104), the Key Research Program in Shaanxi (2017NY-114), and the Fundamental Research Funds for the Central Universities (No. xjj2017102).

Conflicts of interest

There are no conflicts to declare.

Notes and references

1 J. X. Fang, J. Li, C. F. Tian, Q. Q. Gao, X. J. Wang, N. Y. Gao, X. L. Wen, C. S. Ma, H. J. You, Z. L. Yang, Q. H. Xu, Q. H. Xiong, and Z. Y. Li, NPG *Asia Mater.*, 2016, **8**, e323.
2 L. Cheng, C. S. Ma, G. Yang, H. J. You, and J. X. Fang, *J. Mater. Chem. A*, 2014, **2**, 4534.
3 S. R. Nicewarner-Pena, R. G. Freeman, B. D. Reiss, L. He, D. J. Pena, I. D. Walton, R. Cromer, C. D. Keating, and M. J. Natan, *Science*, 2001, **294**, 137.

View Article Online
DOI: 10.1039/C8CE02041H

4 J. X. Fang, L. L. Zhang, J. Li, L. Lu, C. S. Ma, S. D. Cheng, Z. Y. Li, Q. H. Xiong, and H. J. You, *Nat. Commun.*, 2018, **9**, 521.
5 H. J. You, Z. M. Peng, J. B. Wu, and H. Yang, *Chem. Commun.*, 2011, **47**, 12595.
6 Y. Yin and A. P. Alivisatos, *Nature*, 2005, **437**, 664.
7 C. Gao, Y. Hu, M. Wang, M. Chi, and Y. Yin, *J. Am. Chem. Soc.*, 2014, **136**, 7474.
8 Z. B. Yang, L. Zhang, H. J. You, Z. Y. Li, and J. X. Fang, *Part. Part. Syst. Charact.*, 2014, **31**, 390.
9 Y. Yang, J. Zhang, Y. Wei, Q. Chen, Z. Cao, H. Li, J. Chen, J. Shi, Z. Xie, and L. Zheng, *Nano Res.*, 2018, **11**, 656.
10 N. Thomas, and E. Mani, *Phys. Chem. Chem. Phys.*, 2018, **20**, 15507.
11 L. Tang, J. Zhang, L. Dong, Y. Pan, C. Yang, M. Li, Y. Ruan, J. Ma, and H. Lu, *Nanotechnology*, 2018, **29**, 375601.
12 H. J. You, Y. T. Ji, L. Wang, S. C. Yang, Z. M. Yang, J. X. Fang, X. P. Song, and B. J. Ding, *J. Mater. Chem.*, 2012, **22**, 1998.
13 Y. N. Xia, K. D. Gilroy, H. C. Peng, and X. H. Xia, *Angew. Chem.-Int. Edit.*, 2017, **56**, 60.
14 H. J. You, F. L. Zhang, Z. Liu, and J. X. Fang, *ACS Catal.*, 2014, **4**, 2829.
15 X. Lin, S. Lin, Y. L. Liu, M. M. Gao, H. Y. Zhao, B. K. Liu, W. Hasi, and L. Wang, *Langmuir*, 2018, **34**, 6077.
16 H. J. You and J. X. Fang, *Nano Today*, 2016, **11**, 145.
17 J. R. Shimpi, D. S. Sidhaye and B. L. V. Prasad, *Langmuir*, 2017, **33**, 9491.
18 J. A. Manzanares, P. Peljo and H. H. Girault, *J. Phys. Chem. C*, 2017, **121**, 13405.
19 N. Razgoniaeva, M. R. Yang, P. Garret, N. Kholmicheva, P. Moroz, H. Eckard, L. R. Romero, D. Porotnikov, D. Khon, and M. Zamkov, *Chem. Mat.*, 2018, **30**, 1391.
20 S. M. Zhang, L. Zhang, K. Liu, M. Liu, Y. d. Yin, and C. b. Gao, *Mater. Chem. Front.*, 2018, **2**, 1328.
21 B. L. V. Prasad, S. I. Stoeva, C. M. Sorensen and K. J. Klabunde, *Chem. Mater.*, 2003, **15**, 935.
22 P. Lee, and D. Meisel, *J. Phys. Chem.*, 1982, **86**, 3391.
23 Y. Wan, Z. Guo, X. Jiang, K. Fang, X. Lu, Y. Zhang, and N. Gu, *J. Colloid Interface Sci.*, 2013, **394**, 263.
24 F. Ruffino, V. Torrisi, and M. G. Grimaldi, *Physica. E*, 2015, **74**, 388.
25 S. Arcidiacono, N. R. Bieri, D. Poulikakos, and C. P. Grigoropoulos, *Int. J. Multiph. Flow.,* 2004, **30**, 979.
26 B. Ingham, T. H. Lim, C. J. Dotzler, A. Henning, M. F. Toney, and R. D. Tilley, *Chem. Mater.*, 2011, **23**, 3312.
27 M. José-Yacamán, C. Gutierrez-Wing, M. Miki, D.-Q. Yang, K. N. Piyakis, and E. Sacher, *J. Phys. Chem. B*, 2005, **109**, 9703.
28 H. J. You, S. C. Yang, B. J. Ding and H. Yang, *Chem. Soc. Rev.*, 2013, **42**, 2880.
29 Z. M. Peng, H. J. You and H. Yang, *ACS Nano*, 2010, **4**, 1501.
30 H. J. You, W. J. Wang, and S. C. Yang, *ACS Appl. Mater. Interfaces*, 2014, **6**, 19035.
31 H. J. You, X. T. Liu, H. Z. Liu, and J. X. Fang, *CrystEngComm*, 2016, **18**, 3934.
32 A. Gentile, F. Ruffino, and M. G. Grimaldi, *Nanomaterials* 2016, *6*, 110.
33 Y. N. Xia, Y. J. Xiong, B. Lim, and S. E. Skrabalak, *Angew. Chem.-Int. Edit.* 2009, **48**, 60.

View Article Online
DOI: 10.1039/C8CE02041H

Table of Contents

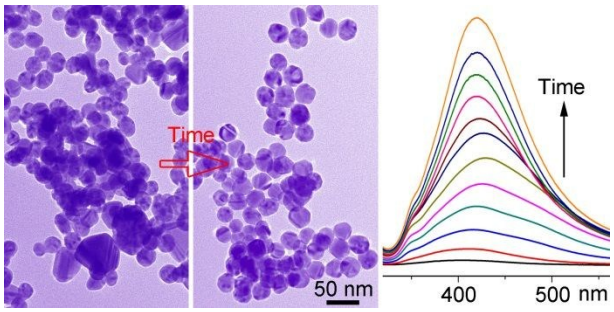

Digestive ripening is introduced into the classical Lee-Meisel synthesis to obtain the uniform and size-controllable Ag nanoparticles.